JOURNAL OF AIRCRAFT
Vol. 40, No. 3, May–June 2003

Thrust Generation Caused by Flapping Airfoils in a Biplane Configuration

Ismail H. Tuncer* and Mustafa Kaya†
Middle East Technical University, 06531 Ankara, Turkey

Unsteady, viscous flows over flapping airfoils in a biplane configuration are computed on moving overset grids. The overset grid solutions are obtained in parallel in a distributed memory environment. Unsteady flowfields are described by particle traces. Time-averaged thrust values are obtained from the integration of the unsteady drag coefficient. It is shown that airfoils in a biplane configuration and oscillating in a combined pitch and plunge motion with a proper phase shift between them produce 20–40% more thrust than a single flapping airfoil. Turbulence in the flow further augments the thrust generation. For a maximum thrust at a given flapping frequency, an optimization of the flapping motion parameters is needed.

Nomenclature

$\bar{C}_t$ = average thrust coefficient,

$$\frac{1}{T}\int_0^T (-C_d)\,\mathrm{d}t$$

c = airfoil chord length (reference length)
f = flapping frequency, hertz
h = instantaneous plunge position
h_0 = nondimensional plunge amplitude
k = reduced frequency $(\omega c/U_\infty)$
T = flapping period, $2\pi/\omega$
t = nondimensional time, $t' U_\infty / c$
t' = dimensional time
U_∞ = freestream velocity
y_0 = mean nondimensional distance between airfoils in a biplane configuration
α = instantaneous incidence angle, deg
α_0 = pitch amplitude, deg
ϕ = phase shift between pitch and plunge oscillations
ω = circular frequency of flapping oscillations, $2\pi f$

Introduction

BASED on the performance of small birds and insects, it appears that flapping wings might be favorable for flights and maneuverability at low Reynolds numbers. Flapping wing propulsion has already been recognized to be more efficient than conventional propellers if applied to very small-scale vehicles, so-called microair vehicles (MAVs). MAVs with wing spans of 15 cm or less and flight speed of 30–60 kph are of current interest for military and civilian applications. Flapping-wing propulsion received considerable attention in the past, but complexity of flapping flight discouraged researchers. There is now a renewed interest in finding the most efficient flapping-wing propulsion technologies to provide required aerodynamic performance for MAV flight.[1]

Recent experimental and computational studies investigated the propulsive characteristics of single and dual flapping airfoils and shed some light on the relationship among the produced thrust, the amplitude, and frequency of the oscillations, and the flow Reynolds number. Water-tunnel flow-visualization experiments on flapping airfoils have been conducted by Lai and Platzer[2] and Jones et al.,[3] which provide a considerable amount of information on the wake characteristics of thrust-producing flapping airfoils. In their experiments Anderson et al.[4] also observed that the phase angle between pitch and plunge oscillations plays a significant role in maximizing the propulsive efficiency. Navier–Stokes computations have been performed by Tuncer and coworkers[5–7] and by Isogai and coworkers[8,9] to explore the effect of flow separation on thrust and propulsive efficiency of a single flapping airfoil in combined pitch and plunge oscillations. Recent experimental studies by Platzer and Jones[10] and by Jones et al.[11,12] with two airfoils arranged in a biplane configuration (Fig. 1) and oscillating in counterphase showed significant thrust and propulsive benefits in comparison to single flapping foils.

In our earlier computational studies[6,7] the flapping motion was implemented by either moving the whole grid with the airfoil or by locally deforming the grid around the moving airfoil. In the biplane configuration (Fig. 2) the grid deformation can impose restrictions on the flapping amplitude, or introduce inaccuracies caused by reduced grid quality. An overset grid system (Fig. 3) is therefore an alternative to impose the flapping motion of airfoils. In addition, overset grid systems readily lend themselves to domain decomposition and parallel computations.

In this study unsteady, viscous flowfields over flapping NACA0014 airfoils in a biplane configuration are computed in parallel on moving overset grids. Parallel computations are carried out in a computer cluster using PVM library routines. The flow over a single flapping airfoil is first computed to validate the overset grid solutions. Laminar and turbulent flows over flapping airfoils in the biplane configuration undergoing pure plunge and combined pitch and plunge are then computed, and the findings are compared with the available experimental and computational data. Conclusions on the thrust enhancement caused by the biplane configuration are drawn.

Numerical Method

The unsteady viscous flowfields are computed by solving the Navier–Stokes equations on overset grids. Computations on each subgrid are performed in parallel. PVM message passing library routines are used in the parallel solution algorithm. The computed flowfields are analyzed in terms of instantaneous distributions of the flow variables, particle traces, and aerodynamic loads.

Navier–Stokes Solver

The strong conservation-law form of the two-dimensional, thin-layer, Reynolds-averaged Navier–Stokes equations is solved on each

Received 22 September 2002; revision received 25 February 2003; accepted for publication 6 March 2003.

*Associate Professor, Department of Aerospace Engineering; tuncer@ae.metu.edu.tr. Member AIAA.

†Graduate Research Assistant, Department of Aerospace Engineering; mkaya@ae.metu.edu.tr.

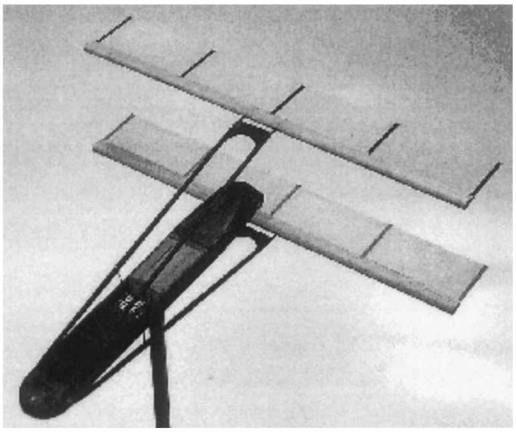

Fig. 1 MAV model.[11]

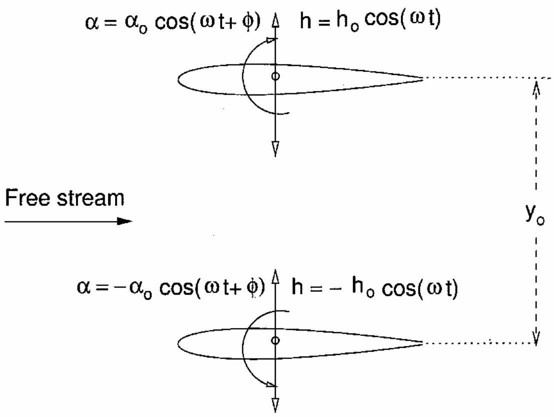

Fig. 2 Out-of-phase flapping motion of two airfoils in a biplane configuration.

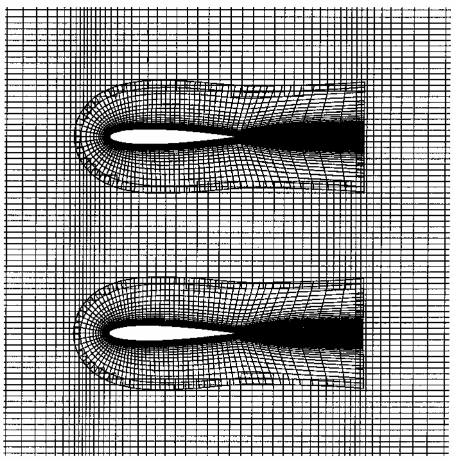

Fig. 3 Overset grid system for a biplane configuration.

subgrid. The governing equations in a curvilinear coordinate system (ξ, ζ) are given as follows:

$$\partial_t \hat{Q} + \partial_\xi \hat{F} + \partial_\zeta \hat{G} = Re^{-1} \partial_\zeta \hat{S} \tag{1}$$

where $\hat{Q}$ is the vector of conserved variables, $1/J(\rho, \rho u, \rho \omega, e)$, $\hat{F}$, and $\hat{G}$ are the convective flux vectors, and $\hat{S}$ is the thin layer approximation of the viscous fluxes in the ζ direction normal to the airfoil surface. The convective fluxes are evaluated using the third-order-accurate Osher's upwind-biased flux-difference-splitting scheme.[7] In turbulent flow computations the Spalart–Allmaras turbulence model is employed.

The discretized equations are solved by an approximately factored, implicit algorithm. The holes in the background grid formed by the airfoil grids are excluded from the computations by an i-blanking algorithm.[13]

Computational Domain

The computational domain is discretized with overset grids. C-type grids around airfoils are overset onto a Cartesian background grid (Fig. 3). The flapping motion of the airfoils is imposed by

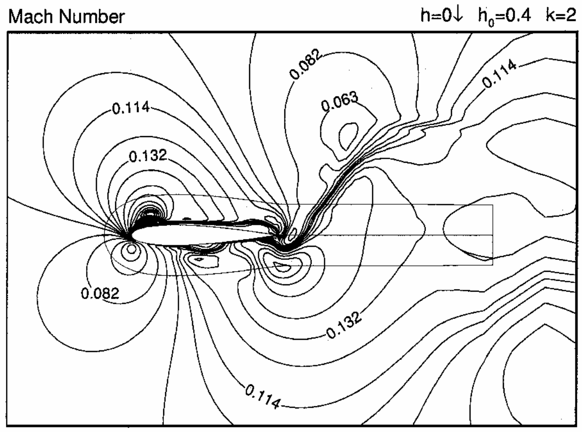

a) Overset grid

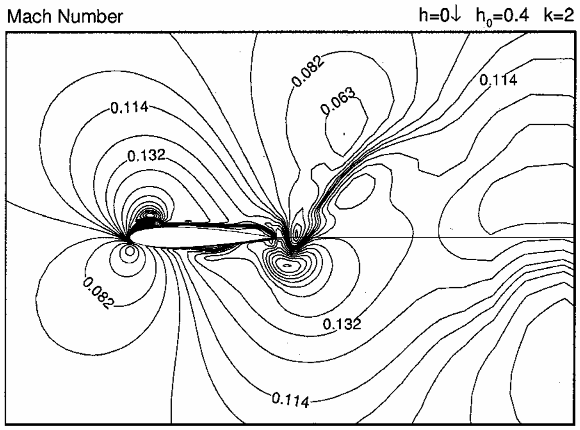

b) Single grid

Fig. 4 Overset and single grid solutions. Unsteady laminar flows are computed at k = 2, h_0 = 0.4, M = 0.1, and Re = 1 × 10^4.

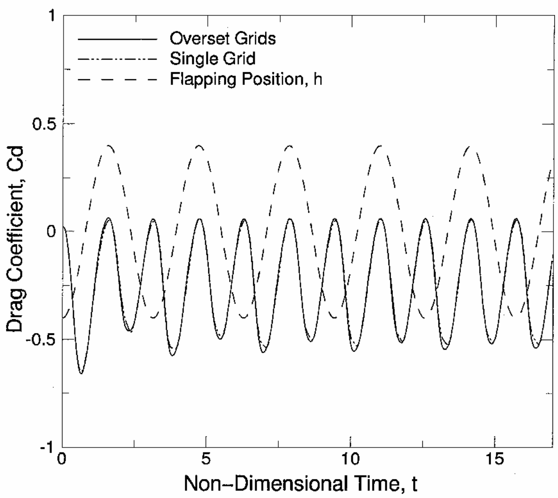

Fig. 5 Unsteady drag coefficient computed at k = 2, h_0 = 0.4, M = 0.1, and Re = 1 × 10^4.

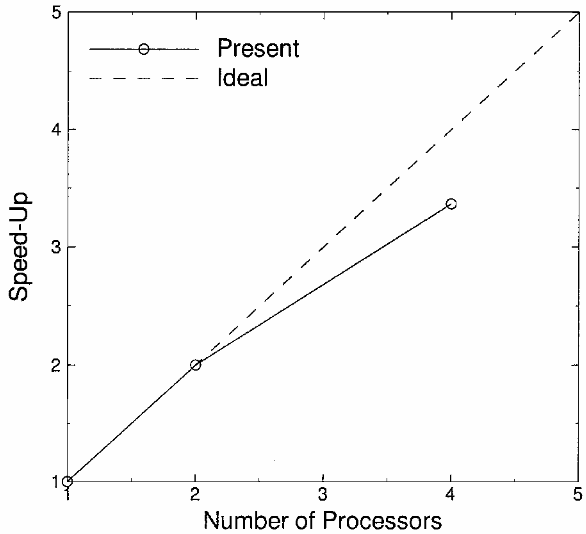

Fig. 6 Parallel efficiency.

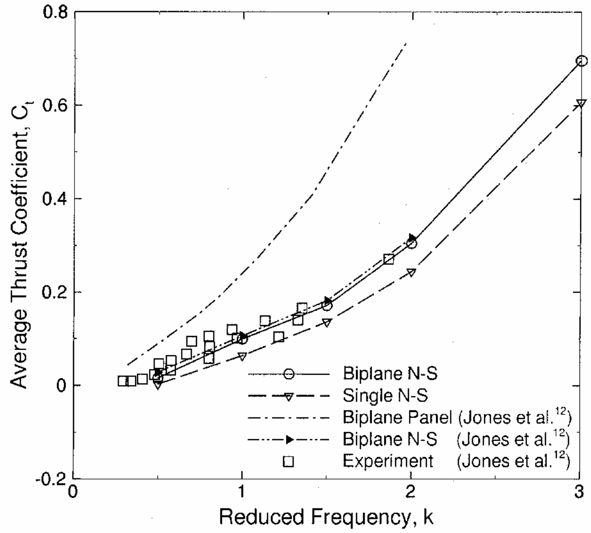

Fig. 8 Average thrust coefficient $h_0 = 0.4, M = 0.1$, and $Re = 1 \times 10^4$.

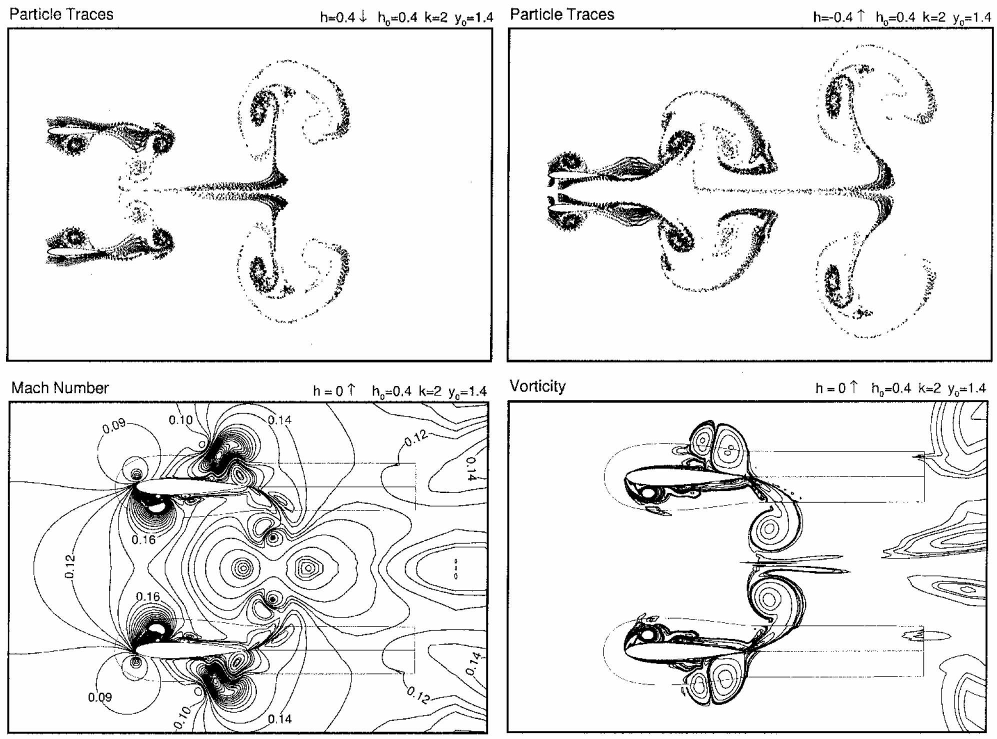

a) Instantaneous flowfield

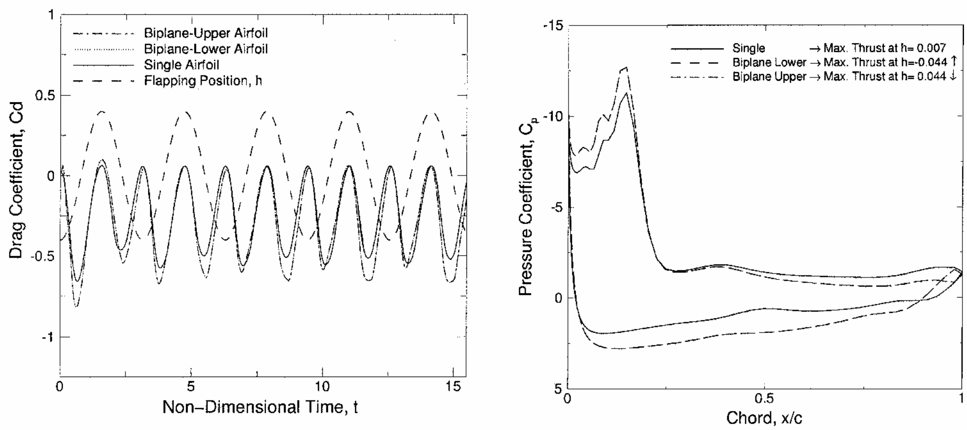

b) Time variation of the drag coefficient and the pressure distribution at the incidence of maximum thrust

Fig. 7 Unsteady laminar flow over flapping airfoils in the biplane configuration computed at $k = 2, y_0 = 1.4, h_0 = 0.4, M = 0.1$, and $Re = 1 \times 10^4$.

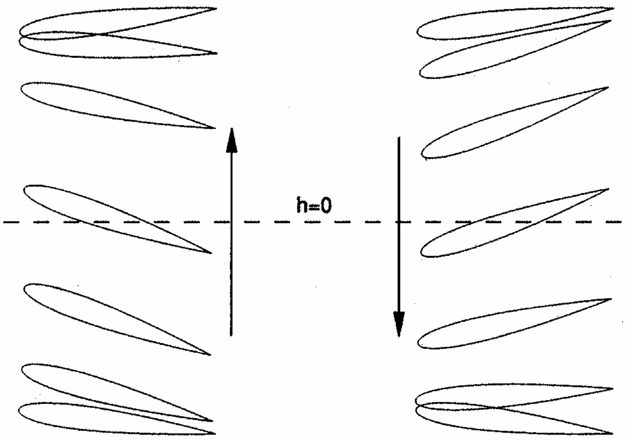

Fig. 9 Combined pitch and plunge motion for ϕ = 100 deg.

moving the airfoils and the computational grids around them over the background grid as specified. The flapping amplitudes of airfoils in plunge and in pitch are defined by

$$h = h_0 \cos(kt), \qquad \alpha = \alpha_0 \cos(kt + \phi) \tag{2}$$

Boundary Conditions

On the airfoil surface the instantaneous flow velocity is set equal to the local surface velocity prescribed by the oscillatory motion [$\dot{h}$, $\dot{\alpha}$ from Eq. (2)], and the no-slip boundary condition is applied. The density and the pressure gradients are also set to zero. At the farfield inflow and outflow boundaries the flow variables are evaluated using the zeroth-order Riemann invariant extrapolation.

At the intergrid boundaries formed by the overset grids, the conserved flow variables are interpolated from the donor grid in each time step of the solution. Intergrid boundary points are first localized in a triangular stencil in the donor grid by a directional search algorithm. The localization process provides the interpolation weights to interpolate the flow variables within the triangular stencil.[13]

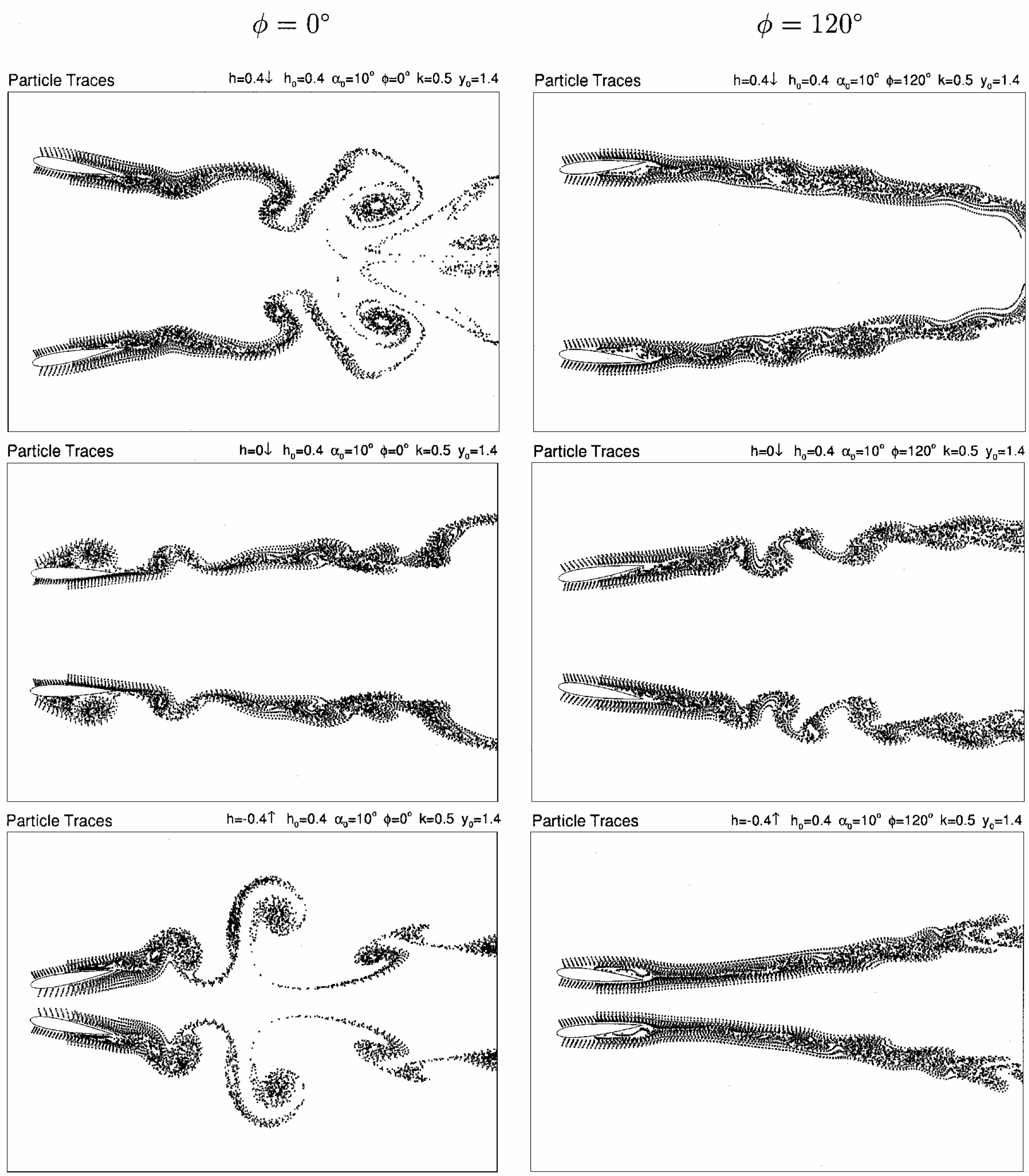

Fig. 10 Unsteady laminar flows over flapping airfoils in combined pitch and plunge computed at $k = 0.5$, $\alpha_0 = 10$ deg, $h_0 = 0.4$, $y_0 = 1.4$, $M = 0.1$, and $Re = 1 \times 10^4$.

Parallel Computation

A parallel solution algorithm based on domain decomposition is implemented in a distributed-memory (computer cluster) environment.[14] The overset grid system is decomposed into its subgrids first, and the solution on each subgrid is assigned to a processor. The background grid can also be partitioned to improve the static load balancing. Intergrid boundary conditions are exchanged among subgrid solutions. PVM (version 3.4.4) library routines are used for interprocess communication. Computations are performed in a cluster of dual-processor (Pentium-III 700MHz) computers running the Linux operating system.

Particle Traces

Particle traces are obtained by a simple and efficient integration of particle pathlines within the flow solver as the unsteady flowfield is computed.[15] In this method particles can be released anywhere in the flowfield at certain intervals. The particles are then localized in the computational grid and convected with the local velocity at every particle path integration time step defined by the user. The particles can be localized across the intergrid boundaries of the overset grids.

Results and Discussion

In this study an overset grid solution with a single flapping airfoil is first validated against the single grid solution. Next, unsteady laminar flows are computed for a biplane configuration as the airfoils are undergoing pure plunge and combined pitch and plunge oscillations in counterphase. A turbulent flow is also studied for comparison. All of the flows are computed at $M = 0.1$ and $Re = 1 \times 10^4$.

An overset grid system for a single flapping NACA0014 airfoil consists of a 141×31 size airfoil grid and a 135×157 size background grid, similar to the one shown in Fig. 3. The flow is computed at $k = 2$, $h_0 = 0.4$. The comparisons of the instantaneous Mach-number distribution and the time variation of the drag coefficient with those of the single grid solution are given in Figs. 4 and 5. The single grid is obtained by expanding the airfoil grid used in the overset grid calculation to the farfield and is of 181×81 size. It is observed that at this high-frequency motion of the airfoil the implementation of the intergrid boundary condition preserves the accuracy of the solution and produces about the same solution as the single grid solution.

In the biplane configuration two NACA0014 airfoils are placed $y_0 = 1.4$ mean distance away from each other and set into the flapping motion in counterphase. The airfoil and background grids are of 141×31 and 135×262 size, respectively. Although the flowfield is symmetric about the midplane in the crossflow direction, the full flow domain is discretized to avoid the application of the numerical symmetry condition and to asses the accuracy of the computations. For parallel computations the background grid is partitioned into two subgrids at the symmetry plane. The computational domain is then decomposed into a total of four subgrids.

The steady flowfield is first computed to provide the starting solution for the unsteady flow. The unsteady flow solutions for a range of reduced frequency values are then computed for about five periods of the flapping motion, in which periodic flow conditions are established. A typical parallel computation, which is distributed over four processors, takes about 20 wall clock hours. The speed up in parallel computations, which is degraded as a result of the unbalanced load distribution, is about 3.4 instead of 4 (Fig. 6). The instantaneous flowfield for $k = 2$ is shown in Fig. 7a. The particle traces, the instantaneous Mach number, and vorticity distributions reveal the presence of large leading- and trailing-edge vortices. The particles are released from 5 and 25 chord locations on the upper and lower airfoil surfaces. The computed flowfield is symmetric about the midplane. The time variation of the drag coefficient and its comparison with that of the single airfoil show that the unsteady thrust production (negative drag) is enhanced in the biplane configuration (Fig. 7b). The instantaneous thrust in the biplane configuration is considerably larger than that of the single airfoil case as the airfoils plunge toward each other at $h \approx 0.\downarrow$ for the upper airfoil ($h \approx 0.\uparrow$ for the lower airfoil). The additional thrust is attributed to the larger

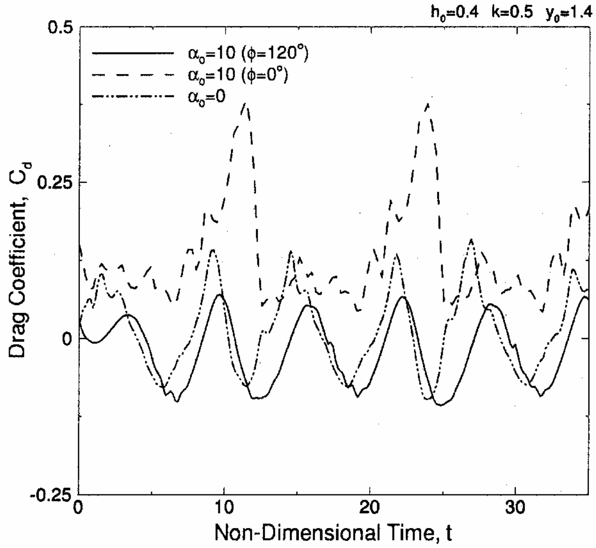

a) Variation of unsteady thrust coefficient

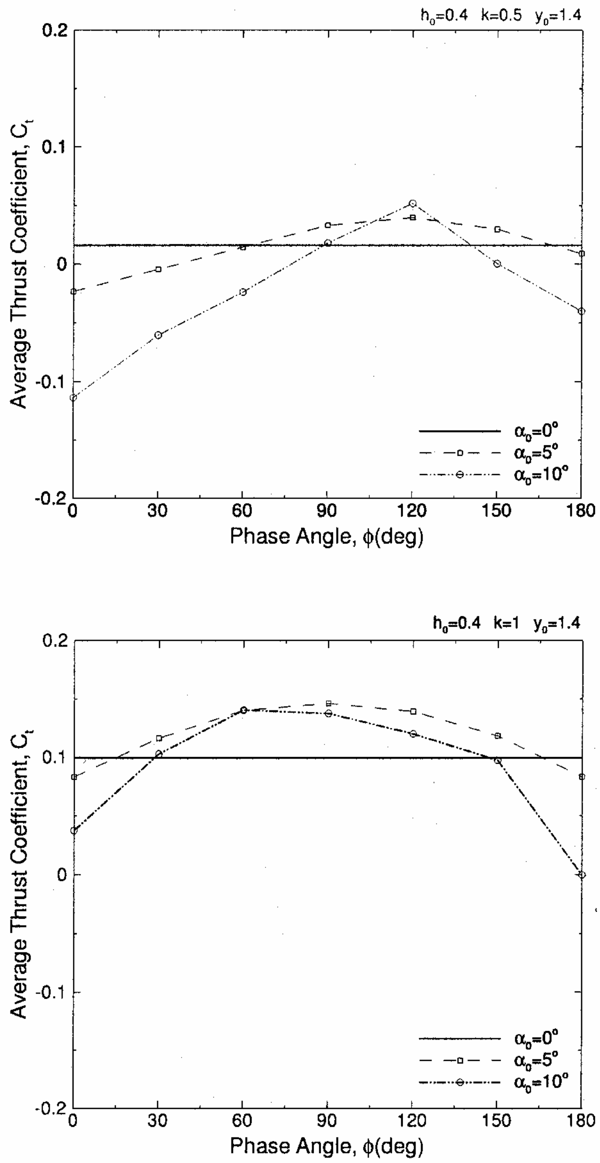

b) Variation of average thrust coefficient

Fig. 11 Variation of thrust coefficient in combined pitch and plunge. Unsteady laminar flows are computed at $h_0 = 0.4, y_0 = 1.4, M = 0.1$, and $Re = 1 \times 10^4$.

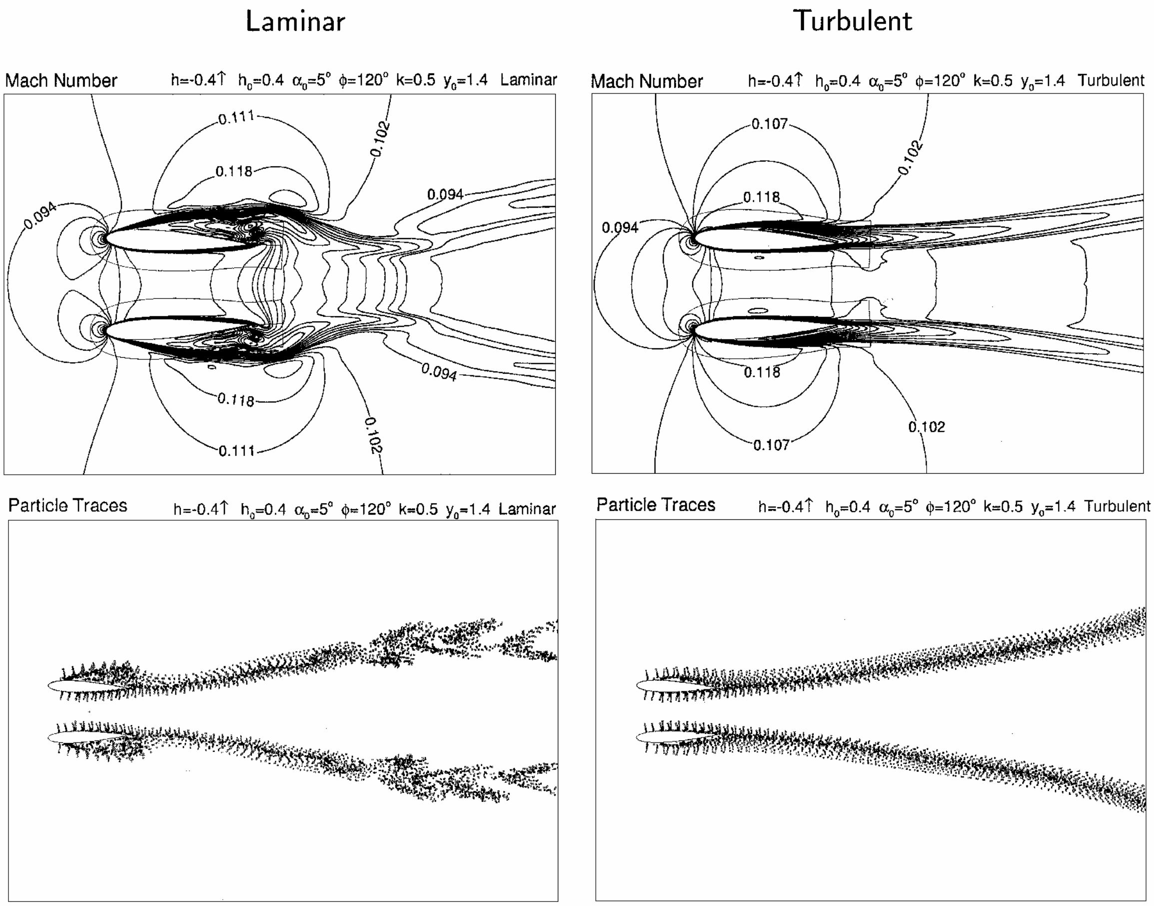

Fig. 12 Unsteady flows over flapping airfoils in combined pitch and plunge computed at k = 0.5, α_0 = 5 deg, ϕ = 10 deg, h_0 = 0.4, y_0 = 1.4, M = 0.1, and $Re = 1 \times 10^4$.

suction at the leading edge of the airfoils as shown in the pressure distributions at the incidence of maximum thrust.

In Fig. 8 the average thrust coefficients (time averaged over a period of the flapping motion), obtained for a range of reduced frequency values $k = 0.5 - 3$, are also compared to those of the single flapping airfoil, the experimental data, and the panel code, and the Navier–Stokes solutions by Jones et al.[12] The Navier–Stokes solutions by Jones et al. are obtained using a single airfoil with a symmetry plane on a deforming C-type grid. In these comparisons the steady-state drag is subtracted from the average thrust as is done in the experimental study. In the experiments the Reynolds number is reported[12] to be less than 2×10^4. Although the experimental data are scattered, the present numerical predictions compare reasonably well with the experimental data. As expected, the panel code solution, which assumes a fully attached flow over airfoils, overpredicts the average thrust considerably. It is observed that the thrust enhancement in biplane configuration becomes more pronounced at high frequencies. For $k > 2$ the enhancement is about 20%.

Finally, the combined pitch and plunge motion (Fig. 9) of the airfoils in the biplane configuration is considered. A set of unsteady flowfields are computed at $y_0 = 1.4, h_0 = 0.4, \alpha_0 = 5, 10$ deg $k = 0.5$, 1.0 and a range of phase angle between $\phi = 0$–180 deg. The particle traces for $\phi = 0$ and 120 deg at $k = 0.5$, $\alpha_0 = 10$ deg are shown in Fig. 10. It is observed that the phase angle ϕ plays a significant role in the development of the flow (Fig. 10) and in the thrust generation (Fig. 11). At $\phi = 0$ deg large leading-edge vortices develop and are shed in to the wake, whereas at $\phi = 120$ deg only small-scale trailing-edge vortices develop. No thrust is generated for $\phi = 0$ deg case (Fig. 11b), whereas the thrust is maximized for $\phi = 120$ deg case. Figure 11a shows that in the case $\phi = 120$ deg the thrust generated during the flapping cycle is sustained longer than it is in the pure plunge case ($\alpha_0 = 0$). Based on the preceding observations, the presence of the large-scale vortices in the flowfield appears to reduce or eliminate the thrust generation.

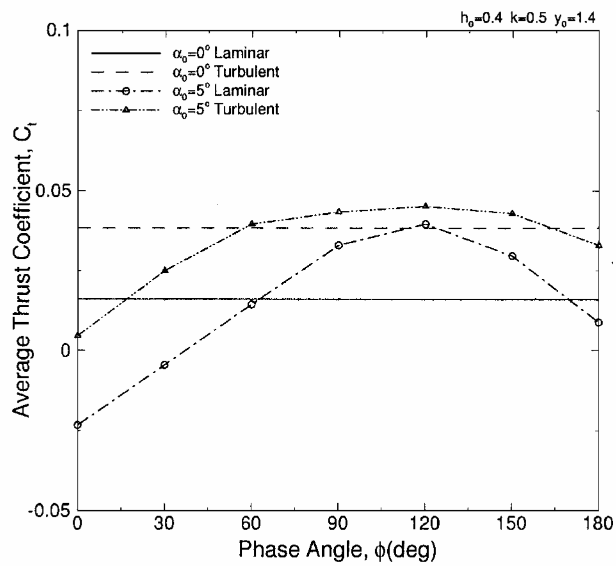

Fig. 13 Variation of thrust coefficient in combined pitch and plunge. Unsteady flows are computed at k = 0.5, h_0 = 0.4, y_0 = 1.4, M = 0.1, and $Re = 1 \times 10^4$.

The average thrust coefficients computed for all of the cases are given in Fig. 11b. It is seen that the thrust produced by flapping airfoils in the biplane configuration might further be increased with the combined pitching motion provided that a proper phase angle is set at 60 deg $< \phi <$ 150 deg. For the phase angles outside of this range, flapping airfoils in pitch and plunge do not produce thrust at all. As the pitch amplitude α_0 increases, the phase angle that maximizes the average thrust slightly shifts, and its proper range narrows down.

The effect of turbulence is next investigated at $k = 0.5$, $\alpha_0 = 0$ deg, 5 deg. The laminar and turbulent flowfields at $\alpha_0 = 5$ deg are shown in Fig. 12. As expected, the turbulent flow delays the flow separation and even prevents the formation of large-scale vortices. As a result, the thrust production in turbulent flows is further enhanced in comparison to the laminar flows (Fig. 13). Although the thrust caused by turbulence increases significantly for the pure plunge case ($\alpha_0 = 0$ deg), the combined pitching motion does not increase the thrust production as significantly as in the laminar flow cases. Based on the preceding cases studied, it can be concluded that the thrust produced by flapping airfoils in the biplane configuration is maximized as the formation of large-scale leading-edge vortices are prevented by either a combined pitching motion with a proper phase angle or by turbulence in the flow.

Conclusions

Unsteady viscous flows over flapping airfoils in a biplane configuration are computed in parallel on overset grids. It is shown that airfoils flapping in a biplane configuration produce 20–40% more thrust than a single flapping airfoil. Thrust production is further enhanced if the airfoils flap in a combined pitch and plunge motion with a proper phase angle between them. It is concluded that the thrust produced by flapping airfoils in a biplane configuration can be maximized as the formation of large-scale vortices are prevented by either a combined pitching motion or by turbulence in the flow. Nevertheless, an optimization of the pitch and plunge parameters, phase angle, reduced frequency, pitch and plunge amplitudes, and the distance between airfoils is needed for maximizing the thrust production.

References

[1]Mueller, T. J. (ed.), *Fixed and Flapping Wing Aerodynamics for Micro Air Vehicles*, Progress in Aeronautics and Astronautics, Vol. 195, AIAA, Reston, VA, 2001.

[2]Lai, J. C. S., and Platzer, M. F., "The Characteristics of a Plunging Airfoil at Zero Free-Stream Velocity," *AIAA Journal*, Vol. 39, No. 3, 2001, pp. 531–534.

[3]Jones, K. D., Dohring, C. M., and Platzer, M. F., "An Experimental and Computational Investigation of the Knoller-Betz Effect," *AIAA Journal*, Vol. 36, No. 7, 1998, pp. 1240–1246.

[4]Anderson, J. M., Streitlien, K., Barrett, D. S., and Triantafyllou, M. S., "Oscillating Foils of High Propulsive Efficiency," *Journal of Fluid Mechanics*, Vol. 360, 1998, pp. 41–72.

[5]Tuncer, I. H., and Platzer, M. F., "Thrust Generation due to Airfoil Flapping," *AIAA Journal*, Vol. 34, No. 2, 1995, pp. 324–331.

[6]Tuncer, I. H., Lai, J., Ortiz, M. A., and Platzer, M. F., "Unsteady Aerodynamics of Stationary/Flapping Airfoil Combination in Tandem," AIAA Paper 97-0659, Jan. 1997.

[7]Tuncer, I. H., and Platzer, M. F., "Computational Study of Flapping Airfoil Aerodynamics," *Journal of Aircraft*, Vol. 35, No. 4, 2000, pp. 554–560.

[8]Isogai, K., Shinmoto, Y., and Watanabe, Y., "Effects of Dynamic Stall on Propulsive Efficiency and Thrust of a Flapping Airfoil," *AIAA Journal*, Vol. 37, No. 10, 2000, pp. 1145–1151.

[9]Isogai, K., and Shinmoto, Y., "Study on Aerodynamic Mechanism of Hovering Insects," AIAA Paper 2001-2470, June 2001.

[10]Platzer, M. F., and Jones, K. D., "The Unsteady Aerodynamics of Flapping-Foil Propellers," *Proceedings of the 9th International Symposium on Unsteady Aerodynamics, Aeroacoustics and Aeroelasticity of Turbomachines*, edited by P. Ferrand and S. Aubert, Presses Universitaires de Grenoble, Grenoble, France, 2001, pp. 123–147.

[11]Jones, K. D., Duggan, S. J., and Platzer, M. F., "Flapping-Wing Propulsion for a Micro Air Vehicle," AIAA Paper 2001-0126, Jan. 2001.

[12]Jones, K. D., Castro, B. M., Mahmoud, O., and Platzer, M. F., "A Numerical and Experimental Investigation of Flapping-Wing Propulsion in Ground Effect," AIAA Paper 2002-0866, Jan. 2002.

[13]Tuncer, I. H., "A 2-D Unsteady Navier–Stokes Solution Method with Moving Overset Grids," *AIAA Journal*, Vol. 35, No. 3, 1997, pp. 471–476.

[14]Tuncer, I. H., "Parallel Computation of Multi-Passage Cascade Flows with Overset Grids," Selected Papers from Parallel Computational Fluid Dynamics Workshop, edited by U. Gulcat and D. R. Emerson, Istanbul Technical Univ., Istanbul, Turkey, 1999, pp. 81–89.

[15]Tuncer, I. H., "A Particle Tracing Method for 2-D Unsteady Flows on Curvilinear Grids," American Society of Mechanical Engineers, Paper FEDSM97-3071, June 1997.